ELSEVIER

Biochimica et Biophysica Acta 1321 (1997) 137–148

BIOCHIMICA ET BIOPHYSICA ACTA
BBA

Fourier transform Raman investigation of the electronic structure and charge localization in a bacteriochlorophyll-bacteriopheophytin dimer of reaction centers from *Rhodobacter sphaeroides*

D. Albouy [a,1], M. Kuhn [b], J.C. Williams [c], J.P. Allen [c], W. Lubitz [b], T.A. Mattioli [a,*]

[a] *Section de Biophysique des Protéines et des Membranes, Département de Biologie Cellulaire et Moléculaire, CEA and URA 2096, C.E. de Saclay, 91191 Gif-sur-Yvette Cedex, France*

[b] *Max-Volmer-Institut für Biophysikalische Chemie und Biochemie, Technische Universität Berlin, Strasse des 17. Juni 135, 10623 Berlin, Germany*

[c] *Department of Chemistry and Biochemistry and Center for the Study of Early Events in Photosynthesis, Arizona State University, Tempe, AZ 85287-1604, USA*

Received 6 March 1997; accepted 22 April 1997

Abstract

The Raman spectra of a bacteriochlorophyll (BChl)-bacteriopheophytin (BPhe) heterodimeric primary electron donor from mutant *Rhodobacter sphaeroides* reaction centers, where histidine M202 has been replaced by leucine, have been obtained in (pre)resonance with its lowest electronic Q_y state using 1064 nm excitation. For reaction centers where the heterodimer is in its reduced, neutral state, the dominant Raman scattering is from the BPhe constituent of the ground state heterodimer, and indicates that the 1064 nm-excitation wavelength is interacting with an electronic state or transition which is largely BPhe in character, such as a charge transfer state with a dominant ($BChl^+BPhe^-$) configuration. Previous electron paramagnetic studies have established that the unpaired electron spin density on the oxidized, cation radical heterodimer resides almost totally on the BChl constituent. Near infrared electronic absorption spectra of the oxidized heterodimer exhibit a weak band at 900 nm, characteristic of a BChl $a^{\cdot+}$ species. The (pre)resonance Raman spectrum of this cation radical, excited at 1064 nm, exhibits a 1723 cm^{-1} band attributable to the C_9 keto carbonyl group of the BChl constituent whose corresponding band in wild type is observed at 1715–1717 cm^{-1}. This 1723 cm^{-1} frequency for BChl in the oxidized heterodimer, compared to 1691 cm^{-1} for the reduced state, represents an oxidation-induced increase in

Abbreviations: (B)Chl, (bacterio)chlorophyll; (B)Phe, (bacterio)pheophytin; *Cf.*, *Chloroflexus*; CT, charge transfer; ENDOR, electron nuclear double resonance; FT, Fourier transform; IR, infrared; P, bacteriochlorophyll dimer primary electron donor; Π, bacteriochlorophyl-bacteriopheophytin 'heterodimer' primary donor; RC, reaction center; RR, resonance Raman; *Rb.*, *Rhodobacter*; *Rps.*, *Rhodopseudomonas*; THF, tetrahydrofuran; Tris, tris(hydroxymethyl)aminomethane

* Corresponding author. Fax: +33 01.69.08.43.89; E-mail: mattioli@dsvidf.cea.fr

[1] Present address: Unité de Physiologie Microbienne, Département de BGM, Institut Pasteur and CNRS 1129, 28 rue du docteur Roux, 75724 Paris cedex 15, France.

PII S0005-2728(97)00044-3

frequency of $+32$ cm^{-1}, similar to what is observed for the one-electron oxidation of chlorophylls in non-protic solvents. The results presented here indicate that the oxidation-induced change in vibrational frequency of the C_9 keto carbonyl group of the BChl in the reaction center is not significantly perturbed by the protein. © 1997 Elsevier Science B.V.

Keywords: Photosynthesis; Heterodimer; Near infrared Fourier transform; Resonance Raman; Chlorophyll oxidation

1. Introduction

The bacterial photosynthetic reaction center (RC) is an integral membrane protein wherein the primary light reactions occur (for reviews, see [1–3]). The three-dimensional crystal structure of RCs from two species of purple bacteria, *Rhodopseudomonas* (*Rps.*) *viridis* and *Rhodobacter* (*Rb.*) *sphaeroides*, have been determined by X-ray diffraction [4–10]. The RC photochemistry and transmembrane charge separation is initiated by the photoexcitation of the primary electron donor P, which is a dimer of bacteriochlorophyll (BChl) molecules in excitonic interaction. The electronic structure and physicochemical properties of the primary donor are critical for the efficient RC functioning (for a recent review, see [11]).

In the RC of *Rhodobacter sphaeroides*, histidines M202 and L173 serve as the axial ligands to each of the bacteriochlorophyll components of P, denoted P_M and P_L, respectively. Genetic substitution of either one of these histidine residues by a leucine residue results in the replacement of the ligated BChl molecule by a bacteriopheophytin (BPhe) instead, thus forming a so-called 'heterodimeric' primary donor (denoted Π) that is still capable of electron transfer (see Fig. 1). The first such heterodimer mutants were constructed in RCs of *Rb. capsulatus* [12] and more recently in those of *Rb. sphaeroides* [13–15]. Electron transfer remains unidirectional along the L branch in these heterodimer mutants but the quantum yield for electron transfer to the primary BPhe acceptor ($BPhe_L$) is lowered from nearly unity, for the wild type RC, to ca. 0.5 [13]. The 'heterodimer' possesses properties quite different from those of the naturally occuring wild type 'homodimer'; there is a 160–180 mV increase in its $\Pi^\circ/\Pi^{\cdot+}$ redox midpoint potential compared to wild type [16,17] and essentially all of the unpaired spin density over $\Pi^{\cdot+}$ is localized on the BChl molecule [14,18,19] resulting in a monomer-like BChl radical cation. In the case of wild type *Rb. sphaeroides*, the unpaired spin density over the two dimer halves in the radical cationic $P^{\cdot+}$ state is delocalized asymmetrically [20] favouring the P_L constituent [21,22].

Resonance Raman spectroscopy is a powerful technique in the investigation of the structure, conformations, protein interactions, and electronic structure of the cofactors in photosynthetic systems. For the study of P, near-infrared Fourier transform (FT) Raman spectroscopy is an ideal vibrational technique because it provides selective, direct vibrational information of P [21,23,24]. This technique, using 1064 nm light excitation, provides preresonance Raman spectra of P via its ca. 860 nm transition, and genuine

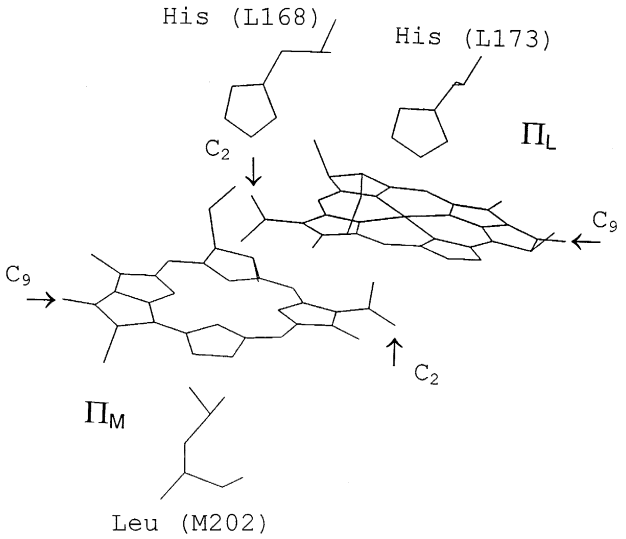

Fig. 1. The three-dimensional structure of the *Rb. sphaeroides* HL(M202) reaction center mutant showing the BChl-BPhe dimer and residues Leu M202, His L173, and His L168. Arrows indicate the C_2 acetyl and C_9 keto carbonyl groups of BPhe (Π_M) and BChl (Π_L) of the heterodimer. The phytl chains and C_{10} carbomethoxy ester carbonyl groups of Π_M and of Π_L have been suppressed for clarity. Residue His L168 is hydrogen bonded to the C_2 acetyl carbonyl group of Π_L. The structure determination was reported in [7] and coordinates are from the Brookhaven National Laboratory Data Bank, File 1PST.

resonance Raman (RR) spectra of the primary donor in its radical cationic $P^{\cdot+}$ state via its 1250 nm absorption band, as described elsewhere [21,23]. The RR spectrum of $P^{\cdot+}$, like ENDOR spectra, provides information concerning the degree of localization of the resulting positive charge (or unpaired electron spin density distribution) over the dimer. This information is obtained directly from measuring the oxidation-induced upshift in vibrational frequency of the C_9 keto carbonyl of one of the BChl components of P, and has been used extensively to estimate this delocalization in mutant RCs of *Rb. sphaeroides* as compared to WT [21,24–26] as well as in other native bacterial reaction centers [27–31]. This type of analysis assumes that the positive charge localization is linear with the upshift and that the upshift in vibrational frequency of the C_9 keto carbonyl observed for the one-electron oxidation of monomeric BChl in non-protic solvents represents 100% localization [21,23].

In this contribution we report the near-infrared Fourier transform Raman spectra of the heterodimeric primary donor from the HL(M202) mutant RC from *Rb. sphaeroides*, in its reduced (Π°) and oxidized ($\Pi^{\cdot+}$) states. In this mutant, the axial ligand, His M202, of the P_M bacteriochlorophyll constituent has been replaced by a leucine residue and a BPhe molecule replaces P_M. Resonance Raman and Fourier transform infrared (FTIR) difference spectroscopic studies of the corresponding HL(M200) reaction center mutant from *Rb. capsulatus* [32–34] and from *Rb. sphaeroides* [35] have been previously reported and a preliminary account of the HL(M202) Π° FT Raman spectrum of the HL(M202) RC mutant of *Rb. sphaeroides* studied here has been presented elsewhere [15]. In this work we specifically report the unusual near-infrared preresonance enhancement of the BPhe molecule within the heterodimer which reflects the mixed BPhe/BChl character its lowest Q_y broad absorption transition at ca. 870 nm. In addition, we determine the vibrational frequency of the $\Pi_L C_9$ keto carbonyl group of the monomer-like BChl radical cation of $\Pi^{\cdot+}$ which shows that its upshift in vibrational frequency, compared to the neutral species, is very similar to that observed in vitro for the one-electron oxidation of BChl *a* or Chl *a* in non-protic solvents [36–38]. The findings in the present paper all indicate that: (i) the HL(M202) mutation in *Rb. sphaeroides* does not significantly alter the pigment–protein interactions of the π-conjugated carbonyl groups of the heterodimer primary donor, consistent with the crystal structure [7] and that the RC protein does not significantly perturb the oxidation-induced vibrational upshift of the keto carbonyl of Π_L; and (ii) vibrational Raman spectroscopy is a reliable technique in analysing the extent of positive charge localization in $P^{\cdot+}$, providing analogous and complementary information normally obtained with other electron paramagnetic techniques.

2. Experimental

The HL(M202) *Rb. sphaeroides* reaction center mutant was constructed by oligonucleotide-directed mutagenesis and cloning of restriction fragments as previously described [14,15]. Reaction center protein was isolated using published procedures found in [15]. RCs were in 0.5% cholate and 20 mM Tris-HCl pH 8 at an O.D. of ca. 150–200 at 800 nm. In this paper, the abbreviation 'WT' RCs denotes those isolated from the deletion strain complemented with the wild type genes, while 'native' RCs refer to those from *Rb. sphaeroides* 2.4.1 or the R-26 carotenoidless strain.

Low-temperature (15 K) Fourier transform Raman measurements were performed on a Bruker IFS 66 interferometer coupled to a FRA 106 Raman module as described elsewhere [21]. Excitation at 1064 nm was provided by a diode-pumped Nd:YAG laser. For near infrared laser excitations other than 1064 nm, a Ti^{4+}:sapphire laser pumped by an Ar^{+} laser was used, as described in [39]. No more than 300 mW of laser power was used in all cases. Samples were held in a cryostat (SMC-TBT, France) whose temperature was regulated by the flow of cold helium gas. For FT Raman spectra of RCs in their neutral Π° state, samples were poised with the addition of ascorbate before freezing in the dark [21]. For the $\Pi^{\cdot+}$ spectra, untreated RC samples were illuminated for ca. 1 min, at room temperature with white light passing through a 10 cm filter of water, then quickly frozen by immersing in liquid nitrogen before transfer to the cryostat [25].

Room temperature near infrared absorption spec-

troscopy was performed using the same FT interferometer as described above, operating in absorption mode [26]. RC samples (1 ml, 0.5 O.D. at 800 nm) were held in a 1 cm quartz cuvette. $P^{\cdot+}$ and $\Pi^{\cdot+}$ absorption spectra were obtained by exploiting the actinic effect of the measuring beam as described elsewhere [25] while for neutral P° and Π° spectra, ascorbate was added, under non-actinic conditions.

3. Results

3.1. Near infrared absorption spectrum of $\Pi^{\cdot+}$

The absorption spectra of the HL(M200) and HL(M202) heterodimer RC mutants of *Rb. capsulatus* and of *Rb. sphaeroides*, respectively, in their reduced Π° state have been discussed in detail elsewhere [12,13,15,40]. In contrast to the well-defined P Q_y absorption band at 865 nm observed for the *Rb. sphaeroides* WT, R-26, and 2.4.1 RCs at room temperature, the analogous band for the HL(M202) mutant is broad with no distinct maximum, apparently centered at ca. 870 nm. In addition, changes are seen in the absorption bands at 540 and 600 nm corresponding to the difference in RC pigment composition [12,13,15].

Fig. 2 compares the room temperature near-infrared electronic absorption spectra of reaction centers from native *Rb. sphaeroides* and the HL(M202) mutant, in their radical cationic $P^{\cdot+}$ and $\Pi^{\cdot+}$ states, respectively. In this figure we note that the 1250 nm (7999 cm^{-1}) band in the homodimer spectrum is absent from that of the heterodimer mutant; this band has been previously assigned to the BChl homodimeric radical cation [41]. The oxidized heterodimer RC mutant exhibits a weaker broad absorption band at 900 nm (11 129 cm^{-1}) and a very weak shoulder at 960 nm (10 430 cm^{-1}). This 900 nm absorption is reminiscent of the corresponding near infrared transition of oxidized monomeric BChl $a^{\cdot+}$ [42] and has been previously tentatively assigned to the monomer-like BChl radical cation in the heterodimer [43]. There are also some differences at ca. 750 nm (ca. 13 333 cm^{-1}) which most probably arise from the different pigment content of the two reaction centers. Fig. 2 also shows that the intense ca. 800 nm (ca. 12 500 cm^{-1}) absorption band is blueshifted for

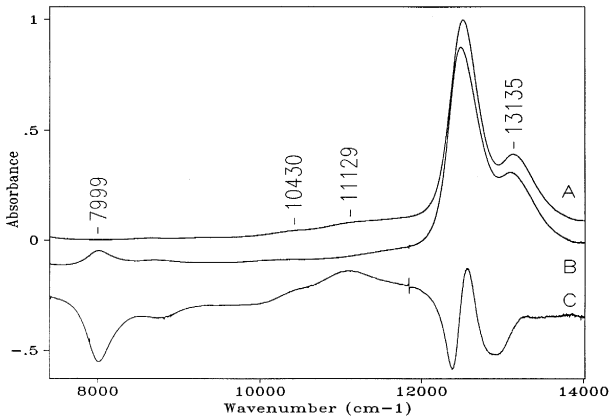

Fig. 2. Room temperature near-infrared electronic absorption spectrum of *Rb. sphaeroides* reaction centers in the $\Pi^{\cdot+}$ and $P^{\cdot+}$ state of (A) the HL(M202) mutant, (B) native, and (C) the calculated difference spectrum (A)-minus-(B) with both spectra normalised at the ca. 800 nm (ca. 12 500 cm^{-1}) absorption band; difference spectrum is $\times 4$. Spectrum B has been shifted down the absorbance scale for pictorial clarity.

the HL(M202) mutant compared to that of the native *Rb. sphaeroides* RCs. For WT RCs in their P° state, the room temperature absorption spectrum exhibits a 804.5 nm band which shifts to 801.9 nm in the $P^{\cdot+}$ state. For the HL(M202) mutant, the corresponding band is observed at 803.2 nm in the Π° state and shifts to 799.2 nm in the $\Pi^{\cdot+}$ state. Thus, the electrochromic blueshift of the 803 nm band for the HL(M202) mutant is 1.3 nm greater than that for the native RC. A similar observation was reported for the HL(200) mutant of *Rb. capsulatus* [43]. This greater blueshift of the heterodimer mutant may be reflecting a more localized charge distribution in the heterodimer exerting a greater field effect on the accessory BChl absorption at ca. 800 nm.

3.2. Near infrared Fourier transform Raman spectroscopy

For WT and native *Rb. sphaeroides* RCs in their reduced P° state, 1064 nm light predominantly enhances the two BChl molecules (P_L and P_M) of 'homodimeric' P to a very similar extent, over the contributions of the accessory BChl and BPhe molecules [21,23]. This is in striking contrast to the HL(M202) heterodimer mutant, for which 1064 nm excitation results in a greater enhancement of the

BPhe molecule within the heterodimer over that of the BChl component when in the Π° state [15] (see also Section 4). This preferential BPhe enhancement is readily observed by the dominant 656 cm^{-1} band in the FT Raman spectrum of the HL(M202) RCs in their Π° state shown in Fig. 3 as compared to that of *Rb. sphaeroides* R-26 RCs in their P° state. This 656 cm^{-1} band is a marker band for BPhe *a* while the band at 735 cm^{-1} is a marker band for BChl *a* [21,23]. This large increase in BPhe contributions to the FT Raman spectrum of the HL(M202) heterodimer mutant compared to native *Rb. sphaeroides* possessing a homodimer is not simply due to the difference in the BChl:BPhe RC pigment ratio. For example, the *Chloroflexus* (*Cf.*) *aurantiacus* RC, in which a BPhe molecule is found in the analogous place of the accessory BChl associated with the M subunit of *Rb. sphaeroides*, possesses a BChl:BPhe pigment ratio of 3:3 as does the HL(M202) *Rb. sphaeroides* mutant RC; the intensity ratio of the BPhe marker band to that of BChl was 0.75 in the P° FT Raman spectrum of reduced *Cf. aurantiacus* RCs compared to 0.25 for those of *Rb. sphaeroides* R-26 [30] while for the HL(M202) mutant RC this ratio is 2.5 (Fig. 3). These ratios not only indicate that the

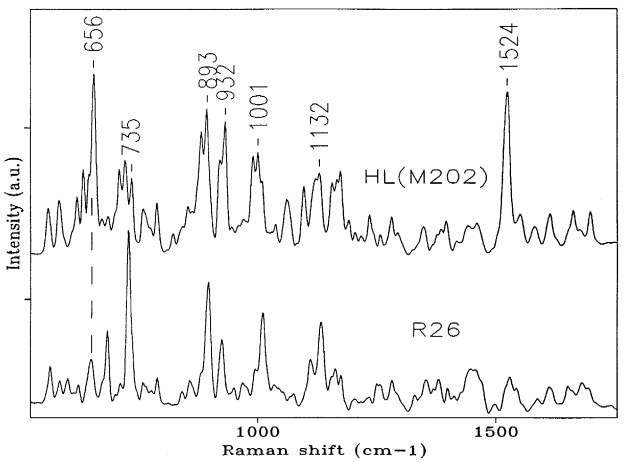

Fig. 3. Low temperature (15 K) FT Raman spectra of reaction centers of *Rb. sphaeroides* carotenoidless R-26 strain and the HL(M202) mutant both in their neutral P° and Π° states, respectively (ascorbate added). The band at 656 cm^{-1} is a marker band for bacteriopheophytin *a*. Experimental conditions: 1064 nm excitation, 250–300 mW laser power, co-addition of 4000 interferograms. The intense bands at 1524, 1001, and 932 cm^{-1} in the HL(M202) spectrum and which are not present in the R-26 spectrum are due to the carotenoid [23] in the HL(M202) RC.

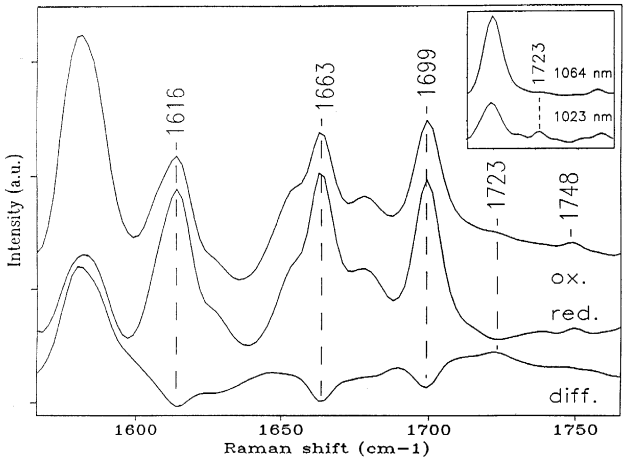

Fig. 4. High frequency region of the 15 K FT Raman spectra of the *Rb. sphaeroides* HL(M202) mutant reaction centers, excited at 1064 nm, in their oxidized (ox.) $\Pi^{\cdot+}$ state (untreated RCs frozen under illumination) and their neutral reduced (red.) Π° state (ascorbate added). Also shown is the calculated $\Pi^{\cdot+}$-minus-Π° spectrum (diff.); this difference spectrum was calculated by normalizing the spectra on the 2900 cm^{-1} band corresponding to the protein and detergent C—H stretching modes. Inset; detail of the 1723 cm^{-1} region of the FT Raman spectra of the RCs in their $\Pi^{\cdot+}$ state excited at 1064 and 1023 nm. Same experimental conditions as in Fig. 3.

Raman scattering of the BPhe of the heterodimer is preresonantly enhanced to a much greater extent than that of the extra monomeric BPhe in the *Cf. aurantiacus* RC [30], they also show that this BPhe dominates the Raman contributions of all the RC pigments, including the BChl constituent of the heterodimer primary donor in the Π° state.

Fig. 4 shows the high frequency region of the FT Raman spectra of RCs of the HL(M202) mutant in its Π° and $\Pi^{\cdot+}$ states; the heterodimer Π° FT Raman spectrum has been previously discussed [15]. The major bands in FT Raman of the HL(M202) mutant RCs in their Π° state are seen at 1616, 1663, and 1699 cm^{-1}. Upon photooxidation these three bands are observed to diminish in intensity, by ca. 40%, unambiguously indicating that they were (pre)resonantly enhanced via the Π° ca. 870 nm transition which itself bleaches upon photooxidation; thus, these FT Raman bands can be assigned confidently as arising from reduced Π°. These Π° bands do not completely bleach as do those of P° in native *Rb. sphaeroides* [21] because of the ca. 50% diminished

yield of $\Pi^{\cdot+}$ formation for the HL(M202) mutant [12,13].

In Fig. 4, observable new bands in the FT Raman spectrum of the HL(M202) mutant in its $\Pi^{\cdot+}$ state are seen at 1723 and 1748 cm^{-1}; these arise because of the concomitant appearance of the ca. 900 nm absorption band via which they are enhanced using 1064 nm excitation and can be assigned confidently to $\Pi^{\cdot+}$. The 1723 cm^{-1} band is more clearly seen in a $\Pi^{\cdot+}$-minus-Π° FT Raman difference spectrum calculated by normalizing the spectra on the 2900 cm^{-1} band of the protein and detergent C—H groups as has been described elsewhere [21,23]. The 1748 cm^{-1} band is similar in frequency to the positive 1751 cm^{-1} band seen in the $\Pi^{\cdot+}$-minus-Π° FTIR difference spectrum of the *Rb. capsulatus* HL(M200) mutant [33,35] and is attributable to the C_{10a} carbomethoxy ester carbonyl of $\Pi^{\cdot+}$. The 1723 cm^{-1} band in the $\Pi^{\cdot+}$ FT Raman spectrum in Fig. 4 is attributable to a C_9 keto carbonyl group of a BChl $a^{\cdot+}$ species; a similar complex feature in the FTIR difference spectrum was seen at ca. 1710–1720 cm^{-1} [33,35]. The relative resonance enhancement of the 1723 cm^{-1} band in Fig. 4 is much weaker than the corresponding 1715–1717 cm^{-1} band in the homodimeric *Rb. sphaeroides* spectrum [21,23,24]. This is to be expected since the heterodimer does not exhibit the characteristic 1250 nm absorption band with which 1064 nm is resonant [21,23]. Since 1064 nm is only preresonant with 900–960 nm band of the heterodimer $\Pi^{\cdot+}$, we would expect its spectrum to be weaker. In addition, due to the diminished efficiency of $\Pi^{\cdot+}$ formation as compared to the WT, we estimate that only ca. 40% of the centers were oxidized under our illumination conditions for the FT Raman experiments. This estimate is derived from the observed ca. 40% lower intensities of the 1616, 1663, and 1699 cm^{-1} bands in the $\Pi^{\cdot+}$ FT Raman spectrum as compared to those of Π° spectrum when these spectra are normalized on the 1524 cm^{-1} carotenoid and ca. 2900 cm^{-1} C—H protein/detergent bands [21,23]. Since the positive charge on the heterodimer is presumed to be localized entirely on the BChl component, we would also expect to observe an upshift of the Π_L C_9 keto carbonyl to be greater for the case of the heterodimer as compared to WT. Indeed, the band at 1723 cm^{-1} is significantly higher in frequency than the 1717 cm^{-1} band observed in *Rb sphaeroides* R-26 and 2.4.1 [21,28], and than the 1715 cm^{-1} band observed in WT [24].

To verify that this weak 1723 cm^{-1} feature is a reliable Raman band, we excited the HL(M202) RCs in their $\Pi^{\cdot+}$ state using various wavelengths of near infrared light. The inset in Fig. 4 shows that changing the excitation wavelength from 1064 nm to 1023 nm for the same sample results in a greater relative enhancement of the 1723 cm^{-1} band; varying the excitation from 1064 to 966 nm (i.e., excitation wavelength approaching the ca. 900 nm absorption band of the $\Pi^{\cdot+}$) resulted in the persistent appearance of the 1723 cm^{-1} band under various degrees of resonant enhancement (data not shown).

4. Discussion

4.1. The BPhe constituent of the heterodimer

The FT Raman data presented above clearly indicate that the 1616, 1663, and 1699 cm^{-1} bands arise from Π° while the 1723 cm^{-1} band arises from $\Pi^{\cdot+}$. Furthermore, the unusually strong preresonant enhancement of the 656 cm^{-1} BPhe marker band in the Π° spectrum indicates that the Raman modes of the BPhe constituent of the heterodimer is greatly enhanced over those of the BChl constituent. Thus, the 1616, 1663, and 1699 cm^{-1} bands of Π° should be those of the BPhe in the heterodimer. The FT Raman contributions of the BChl of the heterodimer in the spectral region shown in Fig. 4 are difficult to directly observe and are masked by the unusually strong BPhe contributions.

In assessing and analysing the FT Raman spectrum in Fig. 4 of the HL(M202) reaction center mutant in its Π° state, it is important to compare the FT Raman spectra of BPhe *a* and BChl *a* in vitro: (i) the C_aC_m methine bridge stretching mode is higher in frequency for BPhe than for pentacoordinated BChl, both at room temperature and at low temperature (10–15K) [21,23,44], (ii) the frequencies of the free C_2 acetyl and free C_9 keto carbonyl stretching frequencies are ca. 13–16 cm^{-1} higher for BPhe than for BChl in the non-hydrogen bonding solvent tetrahydrofuran (THF) [21,23]. Based on the FT Raman spectrum of isolated BPhe *a* in THF, the major bands in the Π° FT Raman spectrum of the HL(M202)

mutant can be assigned. The 1616 cm^{-1} band is assignable to a C_aC_m methine bridge stretching mode of BPhe *a* [21,44]. Indeed, the 1616 cm^{-1} band in Fig. 4 is consistent with it arising from a BPhe molecule since it is 3–4 cm^{-1} higher in frequency than that of the corresponding band for the wild type P_L and P_M BChl cofactors (see point i above) at the same temperature (15 K), which vibrate at 1612–1613 cm^{-1} [45,46]. In addition, the 1663 and 1699 cm^{-1} bands of heterodimer Π° are consistent with the free C_2 acetyl and free C_9 keto carbonyl groups of bacteriochlorin *a* molecules (i.e., BChl *a* and/or BPhe *a*) [21,44]. Unlike the FT Raman spectrum of WT *Rb. sphaeroides* which showed 4 bands attributable to the conjugated carbonyl groups of P (a set of C_2 and C_9 carbonyl bands from each of the two BChl dimer components P_L and P_M), only two bands, corresponding to only one set of C_2 and C_9 carbonyl groups are observed for the heterodimer. This is consistent with only one bacteriochlorin cofactor of the heterodimer being preresonantly enhanced with 1064 nm excitation, over the other RC cofactors, and not two as in the case for the WT homodimer [21,23,24]. Based on the unusually high intensity of the BPhe 656 cm^{-1} marker band in the HL(M202) Π° FT Raman spectrum compared to that of the WT (Fig. 3), the 1663 and 1699 cm^{-1} bands of the Π° heterodimer spectrum must arise from the BPhe within the heterodimer. These frequencies, as stated above, are only consistent with free C_2 and C_9 carbonyl groups, respectively, not engaged in H-bonds and are very similar to what is observed for BPhe *a* in the non-H-bonding solvent THF [21]. This situation is identical to what is observed for the corresponding P_M BChl component in the WT homodimer whose free C_2 and C_9 carbonyl groups vibrate at 1653 and 1680 cm^{-1}, respectively [21,24]. The fact that the C_2 and C_9 carbonyl vibrational frequencies are higher for the heterodimer than for the BChl P_M constituent in the homodimer is also consistent with the assignment that the former arise from the BPhe and not the BChl within the heterodimer (see point (ii) above). The 1663 cm^{-1} band of the free C_2 acetyl carbonyl of the BPhe within the heterodimer agrees well with the resonance Raman assignment to the same carbonyl group of the heterodimer from *Rb. capsulatus*, however the 1699 cm^{-1} band we observe for the C_9 keto carbonyl of this BPhe molecule differs from the 1678

Table 1
Assigned vibrational frequencies (cm^{-1}) for the C_2 and C_9 keto carbonyl groups of the BChls and BPhe (Π_M) of the native and heterodimer primary donors of *Rb. sphaeroides*

	Neutral				Oxidized			
	P_M ($\Pi_M \sim$ [a])		P_L (Π_L)		$P^{\cdot+}$	$\Pi^{\cdot+}$	$\Delta\nu$	$\%P(\Pi)_L$
	C_2	C_9	C_2	C_9	P_LC_9	Π_LC_9	$P(\Pi)_LC_9$ [b]	local. [c]
Native dimer	1653	1679	1620 [d]	1691	1715–1717		+23 [f] − 26 [g]	72–81
Heterodimer	1663	1699	1620 [e]	1691 [e]		1723	+32	100
BPhe *a* [h]	1670	1703						
BChl *a* [h]	1657	1687					+32 [i],32 [j],37 [k]	

[a] BPhe constituent of the heterodimer in the HL(M202) mutant.
[b] Upshift in vibrational frequency of the C_9 keto carbonyl of $P(\Pi)_L$ or of BChl *a* in non-protic solvents.
[c] Percent localization of the resulting positive charge in the oxidized primary donor cation radical. This value is obtained by comparing $\Delta\nu$ with +32 cm^{-1} upshift [21].
[d] The observed vibrational frequency of the C_2 carbonyl group of P_L which is hydrogen bonded; the other vibrational frequencies in this table reflect non-hydrogen bonded carbonyl groups.
[e] Inferred values based on [21,24,25] (see text for details).
[f] From *Rb. sphaeroides* strain in [24].
[g] From *Rb. sphaeroides* strain in [21].
[h] From [21].
[i] Resonance Raman data from [36,38].
[j] Infrared absorption data from [37].
[k] Resonance Raman data from [57].

cm^{-1} band assignment made from RR studies [34]. Our assignments indicate that the conjugated carbonyl groups of BPhe molecule within the heterodimer of *Rb. sphaeroides* are free of H-bond interactions, which is the same situation for the corresponding P_M BChl consitutent of P in the homodimer. Furthermore, these data show that the pigment–protein interactions of the BPhe molecule of the heterodimer are not significantly perturbed and strongly suggest that the replacement of P_M with a BPhe does not significantly alter the geometry and protein interactions of the primary donor within its binding pocket, consistent with the X-ray crystal structure [7]. Our assignments are summarized in Table 1.

4.2. Enhancement of BPhe (Π_M) Raman scattering

The FT Raman spectra of Π° presented in this work and elsewhere [15], using 1064 nm excitation, unambiguously show that the BPhe constituent (Π_M) of the heterodimer is predominantly enhanced. In the simplest representation of the lowest lying excited electronic states of Π, the wavefunctions involved consist of different contributions from the two locally excited configurations (BChl$*$ BPhe) and (BChl BPhe*), and from the two charge transfer (CT) configurations ($BChl^+$ $BPhe^-$) and ($BChl^-$ $BPhe^+$). The (BChl BPhe*) is expected to be higher in energy than the (BChl* BPhe) configuration (based on the fact that the Q_y near-infrared absorption band of BPhe is higher in energy than that of BChl) and is unlikely to be preferentially excited at 1064 nm. In addition, the ($BChl^-$ $BPhe^+$) configuration is expected to be very much higher in energy than the ($BChl^+$ $BPhe^-$) configuration, based on the lower oxidation potential of BChl as compared to that of BPhe [47]. Thus, the preresonant enhancement of BPhe in the FT Raman spectra of Π° most likely arises from the excitation predominantly interacting with the CT state with the ($BChl^+BPhe^-$) configuration.

There could be several possible explanations for a predominant contribution of this CT state upon excitation at the red edge of the heterodimer absorption band. (i) Low-temperature Stark spectroscopy of the broad near-infrared band of the HL(M202) RC mutant reveals two distinct features at ca. 850 and 930 nm [48]. The authors of a resonance Raman study concluded that spectra recorded using excitation wavelengths between 825 and 900 nm were dominated by BChl contributions, and therefore the 850 nm absorption component arises from a state which is largely excitonic in character resulting in enhanced BChl (Π_L) RR scattering [49,50]. If these two absorption features correspond to states having predominantly excitonic or CT character, then the observed enhancement of the BPhe component using 1064 nm excitation would indicate that the lower-energy absorption component (i.e., the 930 nm feature, which is nearer in energy to 1064 nm than is the 850 nm feature) is largely CT in character. This view suggests that the ($BChl^+BPhe^-$) CT configuration of Π^* lies lower in energy than the locally excited (BChl* BPhe) and (BChl BPhe*) configurations, in agreement with the conclusions of a study on the Stark effect in RCs from *Rb. capsulatus* [51]. However, this interpretation of the spectral features is not consistent with other studies that have concluded that the CT state should lie at higher energy than the locally excited state [48,52]. (ii) Another possibility is that electronic states involved are very broad in energy as suggested by the large line width of the absorption band. In that case both the locally excited and CT states could contribute, and the observed enhancement would reflect a greater coupling to the CT state at the energy of the excitation. Recently, Zhou and Boxer [53] have proposed a model in which the 850 and 930 nm low-temperature absorption components of Π result from intermediate charge resonance interactions between the lower molecular excitonic (locally excited) state and a vibronically broad ($BChl^+BPhe^-$) CT state. (iii) A third possibility is that additional states contribute to the absorption features, and that the spectral region at or near the red edge of the absorption band is mainly due to another distinct state with sizable BPhe character.

4.3. The BChl constituent in the oxidized heterodimer $\Pi^{\cdot+}$ cation radical

The 1723 cm^{-1} FT Raman band of $\Pi^{\cdot+}$ (Fig. 4 and inset) is attributable to the vibrational stretching mode of a C_9 keto carbonyl which has upshifted upon oxidation of Π° [21,23]. In the FT infrared absorption $\Pi^{\cdot+}$-minus-Π° difference spectrum of the

HL(M200) mutant of *Rb. capsulatus*, differential features at 1710 and/or 1720 cm^{-1} were tentatively assigned to the C_9 keto carbonyl group of the oxidized heterodimer [33,35]. For the homodimer in *Rb. sphaeroides*, the FT Raman spectrum of $P^{\cdot+}$, the corresponding C_9 keto carbonyl of P_L is seen at 1717 cm^{-1} for R-26 [21] and 2.4.1 [28], and at 1715 cm^{-1} for the WT RC [24]. Thus, the 1723 cm^{-1} band of the heterodimer $\Pi^{\cdot+}$ species is significantly higher in frequency than the corresponding band in the homodimer.

Resonance Raman spectroscopy is a useful technique in analysing the extent of charge distribution in porphyrin radical complexes [54–58]. As previously discussed [21,23–25,28], the upshift of the P_L C_9 keto carbonyl band in the FT Raman spectrum of *Rb. sphaeroides* RCs upon oxidation can be used to estimate the degree of positive charge localization on the P_L constituent of the primary donor. In a simple model we assume that the observed carbonyl vibrational frequency upshift is proportional to the charge localization and that no other protein-induced BChl structural changes affecting the C_9 keto carbonyl frequency occurs as a result of P oxidation. Considering that a non-H-bonded keto carbonyl group of monomeric BChl $a^{\cdot+}$ (one-electron oxidation) *in vitro* upshifts 32 cm^{-1} [36–38], this upshift was taken to represent 100% positive charge localization. For the cases of native *Rb. sphaeroides* strains R-26 and 2.4.1, the 1717 cm^{-1} band represented a 26 cm^{-1} upshift of the P_L C_9 keto carbonyl from 1691 cm^{-1} in the neutral state [21,28] while the 1715 cm^{-1} band in the WT FT Raman spectrum represented a 23–24 cm^{-1} upshift [24]. Within the simple model, we suggested that the 26 cm^{-1} upshift for the cases of *Rb. sphaeroides* R-26 and 2.4.1 indicated that ca. 80% of the positive charge was located on P_L while the 23–24 cm^{-1} upshift seen for the case of WT indicated a 72–75% localization of the positive charge on P_L. In addition, according to our model, we would expect 100% positive charge localization on P_L to give a C_9 carbonyl vibrational frequency of 1691 $cm^{-1} + 32$ $cm^{-1} = 1723$ cm^{-1}.

The oxidation of the heterodimer is to be taken as a monomer-like BChl radical cation of the Π_L constituent [14,18,19] where essentially 100% of the unpaired spin density is on Π_L. Although the frequency of the Π_L C_9 keto carbonyl in the Π° state cannot be directly observed for the HL(M202) mutant, its value should be very similar to that observed for *Rb. sphaeroides* 2.4.1, R-26, and WT which is 1691 cm^{-1}. The X-ray crystal structure of the *Rb. sphaeroides* HL(M202) mutant RC indicates that there should be no major structural changes in the primary donor binding pocket to perturb this carbonyl vibration which is not engaged in a hydrogen bond. Assuming that the Π_L C_9 keto carbonyl vibrates at 1691 cm^{-1} in the Π° state, then the 1723 cm^{-1} band in the heterodimer $\Pi^{\cdot+}$ FT Raman spectrum represents a ca. 32 cm^{-1} upshift of the Π_L C_9 keto carbonyl reflecting the essentially 100% positive charge localization on Π_L. This upshift is very similar to that observed in the one-electron oxidation of BChl *a* in non-protic solvents [36–38]. This result provides good indications that there are no protein conformational changes which makes the oxidation-induced upshift in the keto carbonyl frequency dramatically deviate from in vitro model studies and supports our simple analysis of keto carbonyl frequency upshift and positive charge localization.

We have noted in some other mutants of *Rb. sphaeroides* where more drastic changes in the P binding pocket were genetically introduced such as adding or removing histidine residues which formed or ruptured H-bonds to the C_2 and C_9 keto carbonyl groups of P, but where the P_L C_9 keto carbonyl was not a target, that secondary effects introduced frequency shifts of this latter carbonyl group ranging from -3 to $+5$ cm^{-1}; the largest shifts resulted from multiple point mutations [25,26]. Considering: (i) the lack of evidence for significant structural changes in the Π binding pocket, based on the X-ray crystal structure of the *Rb. sphaeroides* HL(M202) mutant and the above discussion; and (ii) the relatively less drastic single point mutation of HL(M202) which results in the incorporation of BPhe into the primary donor binding pocket, compared to the more drastic multiple point mutations which directly changes the protein–H-bond interactions with P which could indirectly alter the P_L C_9 carbonyl vibrational frequency by as high as 5 cm^{-1}, then we expect that the error in our calculated upshift of 32 cm^{-1} for the P_L C_9 keto carbonyl in the HL(202) mutant in the $\Pi^{\cdot+}$ state is less than ± 3 cm^{-1}.

Recently, Diers and Bocian [59] suggested that the assumption that the vibrational frequency shift is

linear with the degree of positive charge localization on the macrocycle may not be valid. The work presented here provides good support for the validity of this assumption. For the case of the HL(M202) mutant, the protein does not appear to significantly perturb the BChl macrocycle and the oxidation-induced upshift of the C_9 keto carbonyl vibrational frequency of 32 cm^{-1} is conserved whether in the protein or in a non-protic solvent. Thus, the 1723 cm^{-1} Raman band seen for the C_9 keto carbonyl of P_L in the $\Pi^{\cdot+}$ spectrum is consistent with what one would expect for the 32 cm^{-1} shift of the 1691 cm^{-1} band in the Π° spectrum.

For the WT *Rb. sphaeroides* RCs in their $P^{\cdot+}$ state, our FT Raman results on the positive charge localization on P_L (72–75%) are in qualitative agreement with ENDOR measurements (68%) [14,24]. Similar qualitative agreement was also seen in a series of *Rb. sphaeroides* mutant RCs [14,24,25]. In the FT Raman analysis, the C_9 keto carbonyl of P_L is used to gauge the localization on P_L while for the ENDOR experiments the protons of the CH_3 methyl groups at the C_1 and C_5 positions of both BChls of P are used as the probes of the spin density distribution over the P_L macrocycle. Considering the different physical bases of the ENDOR and the Raman experiments, as well as the different locations on the BChl macrocycle of the group probes used in the two experiments, it is remarkable that qualitative agreements are observed. Based on our observations in this paper that 100% localization of the positive charge on Π_L results in an upshift of the keto carbonyl group that is very similar to that observed in vitro in non-H-bonding solvents, we have excluded the possibility that protein factors significantly influence this upshift and, thus, misleading our determination of positive charge localization in the oxidized primary donor. In reconciling an exact quantitative agreement between the FT Raman and the ENDOR data perhaps the limiting assumption is whether the unpaired spin density observed in the chemical group probes (i.e., CH_3 and $C=O$) reflect a homogeneous spin density throughout the macrocycle. The fact that the C_9 keto carbonyl is conjugated to the π-system of the entire BChl macrocycle, and that this carbonyl group is not susceptible to the same geometric variations (i.e., angular variations with the plane of the macrocycle) as the C_2 acetyl carbonyl, then the C_9 keto carbonyl group should constitute a good probe.

In summary, the observation of the C_9 keto carbonyl group of the BChl constituent of the heterodimer vibrating at 1723 cm^{-1}, which bears essentially 100% of the unpaired spin density (or positive charge) in the heterodimer $\Pi^{\cdot+}$, strongly suggests that this carbonyl group undergoes very similar oxidation-induced vibrational upshifts in frequency to those observed for BChl and Chl in non-hydrogen bonding solvents, and that there are no dramatic protein conformational changes which cause the observed upshift to significantly deviate from the $+32$ cm^{-1} upshift of the same keto carbonyl in the one-electron oxidation of BChl *a* in non-H-bonding solvents. Thus, our vibrational analysis of using this upshift in estimating the degree of positive charge localization in dimeric primary donors in other mutant or native reaction centers appears based on valid assumptions.

Acknowledgements

We thank X. Nguyen for preparation of reaction centers and Dr. A. Ivancich for stimulating discussions, as well as Prof. Steve Boxer for communicating material prior to publication. J.P.A. and J.C.W. gratefully acknowledge support from NSF (MCB9404925) and W.L. from Deutsche Forschungsgemeinschaft (Sonderforschungsbereich 312, TP A4) and Fonds der Chemischen Industrie.

References

[1] W.W. Parson, in: H. Scheer (Ed.), Chlorophylls, CRC Press, Boca Raton, FL, 1991, pp. 1153–1180.
[2] C. Kirmaier, D. Holten, in: J. Deisenhofer, J.R. Norris (Eds.), The Photosynthetic Reaction Center, vol. II, pp 49–70, Academic Press, San Diego, 1993.
[3] N.W. Woodbury, J.P. Allen, in: R.E. Blankenship, M.T. Madigan, C.E. Bauer (Eds.), Anoxygenic Photosynthetic Bacteria, Kluwer, Dordrecht, The Netherlands, 1995, pp. 527–557.
[4] J. Deisenhofer, O. Epp, K. Miki, R. Huber, H. Michel, Nature 318 (1985) 618–624.
[5] J.P. Allen, G. Feher, T.O. Yeates, H. Komiya, D.C. Rees, Proc. Natl. Acad. Sci. U.S.A. 84 (1987) 5730–5734.

[6] O. El-Kabbani, C.-H. Chang, D. Tiede, J. Norris, M. Schiffer, Biochemistry 30 (1991) 5361–5369.
[7] A.J. Chirino, E.J. Lous, M. Huber, J.P. Allen, C.C. Schenck, M.L. Paddock, G. Feher, D.C. Rees, Biochemistry 33 (1994) 4584–4593.
[8] U. Ermler, G. Fritzsch, S.K. Buchanan, H. Michel, Structure 2 (1994) 925–936.
[9] J. Deisenhofer, O. Epp, I. Sinning, H. Michel, J. Mol. Biol. 246 (1995) 429–457.
[10] B. Arnoux, F. Reiss-Husson, Eur. Biophys. J. 24 (1996) 233–242.
[11] J.P. Allen, J.C. Williams, J. Bioenerg. Biomemb. 27 (1995) 275–283.
[12] E.J. Bylina, D.C. Youvan, Proc. Natl. Acad. Sci. U.S.A. 85 (1988) 7226–7230.
[13] L.M. McDowell, D. Gaul, C. Kirmaier, D. Holten, C.C. Schenck, Biochemistry 30 (1991) 8315–8322.
[14] J. Rautter, F. Lendzian, C. Schulz, A. Fetsch, M. Kuhn, X. Lin, J.C. Williams, J.P. Allen, W. Lubitz, Biochemistry 34 (1995) 8130–8143.
[15] J.P. Allen, K. Artz, X. Lin, J.C. Williams, A. Ivancich, D. Albouy, T.A. Mattioli, A. Fetsch, M. Kuhn, W. Lubitz, Biochemistry 35 (1996) 6612–6619.
[16] D. Davis, A. Dong, W.S. Caughey, C.C. Schenck, Biophys. J. 61 (1992) A153.
[17] L. Laporte, L.M. McDowell, C. Kirmaier, C.C. Schenck, D. Holten, Chem. Phys. 176 (1993) 615–629.
[18] E.J. Bylina, S.V. Kolaczkowski, J.R. Norris, D.C. Youvan, Biochemistry 29 (1990) 6203–6210.
[19] M. Huber, R.A. Isaacson, E.C. Abresch, D. Gaul, C.C. Schenck, G. Feher, Biochim. Biophys. Acta 1273 (1996) 108–128.
[20] F. Lendzian, B. Endeward, M. Plato, D. Bumann, W. Lubitz, K. Möbius, K., in: M.E. Michel-Beyerle (Ed.), Reaction Centers of Photosynthetic Bacteria, Springer, Berlin, 1990, pp. 57–68.
[21] T.A. Mattioli, A. Hoffmann, B. Robert, B. Schrader, M. Lutz, Biochemistry 30 (1991) 4648–4654.
[22] F. Lendzian, M. Huber, R.A. Isaacson, B. Endeward, M. Plato, B. Bönigk, K. Möbius, W. Lubitz, Biochim. Biophys. Acta 1183 (1993) 139–160.
[23] T.A. Mattioli, A. Hoffmann, D.G. Sockalingum, B. Schrader, B. Robert, M. Lutz, Spectrochim. Acta 49A (1993) 785–799.
[24] T.A. Mattioli, J.C. Williams, J.P. Allen, B. Robert, Biochemistry 33 (1994) 1636–1643.
[25] T.A. Mattioli, X. Lin, J.P. Allen, J.C. Williams, Biochemistry 34 (1995) 6142–6152.
[26] J. Wachtveitl, J.W. Farchaus, R. Das, M. Lutz, B. Robert, T.A. Mattioli, Biochemistry 32 (1993) 12875–12886.
[27] I. Agalidis, B. Robert, T.A. Mattioli, F. Reiss-Husson, in: J. Breton, A. Verméglio (Eds.), The Photosynthetic Bacteral Reaction Center II, Plenum, New York, 1992, pp. 133–139.
[28] T.A. Mattioli, B. Robert, M. Lutz, in: J. Breton and A. Verméglio (Eds.), The Photosynthetic Bacterial Reaction Center II, Plenum Press, New York, 1992, pp. 127–132.
[29] U. Feiler, D. Albouy, B. Robert, T.A. Mattioli, Biochemistry 34 (1995) 1099–1105.
[30] A. Ivancich, R. Feick, A. Ertlmaier, T.A. Mattioli, Biochemistry 35 (1996) 6126–6135.
[31] A. Ivancich, M. Kobayashi, F. Drepper, I. Fathir, S. Takauki, T. Nozawa, T.A. Mattioli, Biochemistry 35 (1996) 10529–10538.
[32] J.M. Peloquin, E.J. Bylina, D.C. Youvan, D.F. Bocian, Biochemistry 29 (1990) 8417–8424.
[33] E. Nabedryk, S.J. Robles, E. Goldman, D.C. Youvan, J. Breton, Biochemistry 31 (1992) 10852–10858.
[34] V. Palaniappan, D.F. Bocian, Biochemistry 34 (1995) 11106–11116.
[35] E. Nabedryk, J. Breton, M. Kuhn, A. Fetsch, C. Schulz, W. Lubitz, Biophys. J. 68 (1995) A93 (abstract).
[36] T.M. Cotton, K.D. Parks, R.P. Van Duyne, J. Am. Chem. Soc. 102 (1980) 6399–6407.
[37] W.G. Mäntele, A.M. Wollenwebber, E. Nabedryk, J. Breton, Proc. Natl. Acad. Sci. U.S.A. 85 (1988) 8468–8472.
[38] R.L. Heald, T.M. Cotton, J. Phys. Chem. 94 (1990) 3968–3975.
[39] T.A. Mattioli, J. Mol. Structure 347 (1995) 450–466.
[40] C. Kirmaier, D. Holten, E.J. Bylina, D.C. Youvan, Proc. Natl. Acad. Sci. U.S.A. 85 (1988) 7562–7566.
[41] P.L. Dutton, K.J. Kaufmann, B. Chance, P.M. Rentzepis, FEBS Lett. 60 (1975) 275–280.
[42] J. Fajer, D.C. Borg, A. Forman, R.H. Felton, D. Dolphin, H. Vegh, Proc. Natl. Acad. Sci. U.S.A. 71 (1974) 994–998.
[43] J. Breton, E.J. Bylina, D.C. Youvan, Biochemistry 28 (1989) 6423–6430.
[44] M. Lutz, in: R.J.H. Clark, R.E. Hester (Eds.), Advances in Infrared and Raman Spectroscopy, vol. 11, Wiley, New York, 1984, pp. 211-300.
[45] T.A. Mattioli, D. Sockalingum, M. Lutz, B. Robert, in: N. Murata (Ed.), Research in Photosynthesis Vol. I, Kluwer Academic Publishers, Dordrecht, The Netherlands, 1992, pp. 405–408.
[46] A. Ivancich, M. Lutz, T.A. Mattioli, Biochemistry 36, (1997) 3242–3253.
[47] T. Watanabe, M. Kobayashi, in: H. Scheer (Ed.), Chlorophylls, CRC Press, Boca Raton, FL, 1991, pp. 287–315.
[48] S.L. Hammes, L. Mazzola, S.G. Boxer, D.F. Gaul, C.G. Schenck, Proc. Natl. Acad. Sci. U.S.A. 87 (1990) 5682–5686.
[49] L.L. Laporte, V. Palaniappan, D.G. Davis, C. Kirmaier, C.C. Schenck, D. Holten, D.F. Bocian, J. Phys. Chem. 100 (1996) 17696–17707.
[50] V. Palaniappan, C.C. Schenck, D.F. Bocian, J. Phys. Chem. 99 (1995) 17049–17058.
[51] T.J. DiMagno, E.J. Bylina, A. Angerhofer, D.C. Youvan, J.R. Norris, Biochemistry 29 (1990) 899–907.

[52] E.J.P. Lathrop, R.A. Friesner, J. Phys. Chem. 98 (1994) 3056–3066.
[53] H. Zhou, S.G. Boxer, J. Phys. Chem. (1997) submitted.
[54] P.G. Bradley, N. Kress, B.A. Hornberger, R.F. Dallinger, W.H. Woodruff, J. Am. Chem. Soc. 103 (1981) 7441–7446.
[55] S.M. Angel, M.K. DeArmond, R.J. Donohoe, K.W. Hanck, D.W. Wertz, J. Am. Chem. Soc. 106 (1984) 3688–3689.
[56] R.J. Donohoe, D.F. Bocian, J. Am. Chem. Soc. 112 (1990) 8807–8811.
[57] J.K. Duchowski, D.F. Bocian, Inorg. Chem. 29 (1990) 4158–4160.
[58] T.-H. Tran-Thi, T.A. Mattioli, D. Chabach, A. de Cian, R. Weiss, J. Phys. Chem. 98 (1994) 8279–8288.
[59] J.R. Diers, D.F. Bocian, J. Phys. Chem. 98 (1995) 12884–12892.